Reaction Force and Its Link to Diabatic Analysis: A Unifying Approach to Analyzing Chemical Reactions

DATASET · JANUARY 2010

4 AUTHORS, INCLUDING:

Jeffrey Reimers
University of Technology Sydney
215 PUBLICATIONS **6,682** CITATIONS
SEE PROFILE

Jane S Murray
University of New Orleans
282 PUBLICATIONS **11,702** CITATIONS
SEE PROFILE

Alejandro Toro-Labbé
Pontifical Catholic University of Chile
223 PUBLICATIONS **4,365** CITATIONS
SEE PROFILE

THE JOURNAL OF PHYSICAL CHEMISTRY Letters

pubs.acs.org/JPCL

Reaction Force and Its Link to Diabatic Analysis: A Unifying Approach to Analyzing Chemical Reactions

Peter Politzer,[†] Jeffrey R. Reimers,[‡] Jane S. Murray,*[,†] and Alejandro Toro-Labbé[§]

[†]CleveTheoComp LLC, 1951 West 26th Street, Suite 409, Cleveland, Ohio 44113, [‡]School of Chemistry, The University of Sydney, NSW 2006, Australia, and [§]Laboratorio de Química Teórica Computacional (QTC), Facultad de Química, Pontificia Universidad Católica de Chile, Vicuña Mackenna 4860, Casilla 306, Correo 22, Santiago, Chile

ABSTRACT The reaction force $\mathbf{F}(\mathbf{R})$ and the reaction force constant $\kappa(\mathbf{R})$ provide a rigorously based approach to characterizing a chemical process. The energies associated with its different stages are presented and discussed for a number of examples. Analysis of these suggests an alternative, modified expression for the Hammond−Leffler postulate. We show that diabatic analysis leads to a description of the process that is qualitatively very similar to that coming from $\mathbf{F}(\mathbf{R})$ and $\kappa(\mathbf{R})$, quantitatively so for proton-transfer reactions. Reaction force analysis provides a unifying framework that can encompass a variety of independent concepts relating to chemical processes.

SECTION Molecular Structure, Quantum Chemistry, General Theory

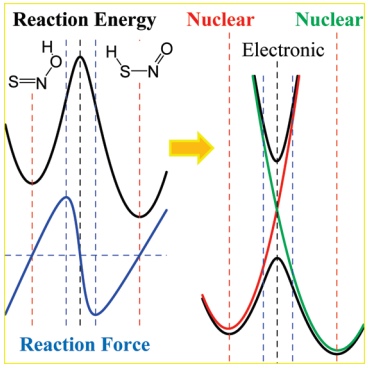

Derivatives of the Potential Energy $V(\boldsymbol{R})$. A traditional means of depicting the course of a chemical process is by showing the variation of its potential energy surface for nuclear motion, $V(\mathbf{R})$, along some appropriate pathway $\mathbf{R}$ from reactants to products. A typical $V(\mathbf{R})$ profile for a one-step conversion of reactants A to products B is in Figure 1a. Such a $V(\mathbf{R})$ plot can be used to determine the activation barrier for the process and the overall gain or release of energy accompanying it. (The discussion to follow does not depend upon whether the process is endothermic or exothermic.)

In recent years, it has been demonstrated that considerable additional information and insight can be obtained from the first and second derivatives of $V(\mathbf{R})$ along $\mathbf{R}$, which is generally taken to be the intrinsic reaction coordinate.[1,2] The negative of the first derivative yields the classically defined reaction force $\mathbf{F}(\mathbf{R})$[3,4]

$$\mathbf{F}(\mathbf{R}) = -\frac{\partial V(\mathbf{R})}{\partial \mathbf{R}} \tag{1}$$

while the second derivative gives the reaction force constant $\kappa(\mathbf{R})$[5,6]

$$\kappa(\mathbf{R}) = \frac{\partial^2 V(\mathbf{R})}{\partial \mathbf{R}^2} = -\frac{\partial \mathbf{F}(\mathbf{R})}{\partial \mathbf{R}} \tag{2}$$

For the $V(\mathbf{R})$ in Figure 1a, the corresponding $\mathbf{F}(\mathbf{R})$ and $\kappa(\mathbf{R})$ are shown in Figure 1b and c. Their features are dictated solely by the form of $V(\mathbf{R})$.

In this Letter, we shall examine the relationships between the energy changes in the various stages of a chemical reaction. We will also demonstrate that the characterization of a process that is provided by $\mathbf{F}(\mathbf{R})$ and $\kappa(\mathbf{R})$ is linked qualitatively and quantitatively to the description obtained independently from diabatic analysis.

Reaction Force. Figure 1b shows that $\mathbf{F}(\mathbf{R})$ has a minimum at R_α and a maximum at R_γ. These features define a rigorous partitioning of the process into three regions. The first is prior to the $\mathbf{F}(\mathbf{R})$ minimum, from R_A to R_α; the second is between the minimum at R_α and the maximum at R_γ; and the third is after the maximum, from R_γ to R_B. Investigation of a series of reactions of different types has shown that certain general characteristics are associated with each of these regions. The reactions studied include S_N2 substitution,[7−9] addition to double bonds,[10,11] bond dissociation,[12−14] proton transfer,[15−17] nitro/aci tautomerization,[18] and molecular rearrangements.[19]

What was observed in detailed studies of these reactions is that the first region, from R_A to R_α, usually emphasizes structural changes in the reactants — bond stretching, rotations, angle bending, and so forth. $\mathbf{F}(\mathbf{R})$ reflects the resistance to these changes and therefore becomes increasingly negative, that is, retarding, reaching its extremum at R_α, at which point the system can generally be regarded as distorted (activated) states of the reactants.

It is in the second region, between R_α and R_γ, that the major portion of the transition to products normally takes place and that electronic factors are most important. Bonds break and form, there are often rapid and extensive changes in properties such as the electrostatic potential, and so forth. The reaction force $\mathbf{F}(\mathbf{R})$ now includes a growing driving component that gradually counteracts the resistance and becomes dominant after the point R_β, which corresponds to the maximum of $V(\mathbf{R})$. At R_γ, the maximum of $\mathbf{F}(\mathbf{R})$, the system can frequently be viewed as distorted (activated)

Received Date: August 12, 2010
Accepted Date: September 7, 2010
Published on Web Date: September 14, 2010

DOI: 10.1021/jz101135y | *J. Phys. Chem. Lett.* **2010**, *1*, 2858–2862

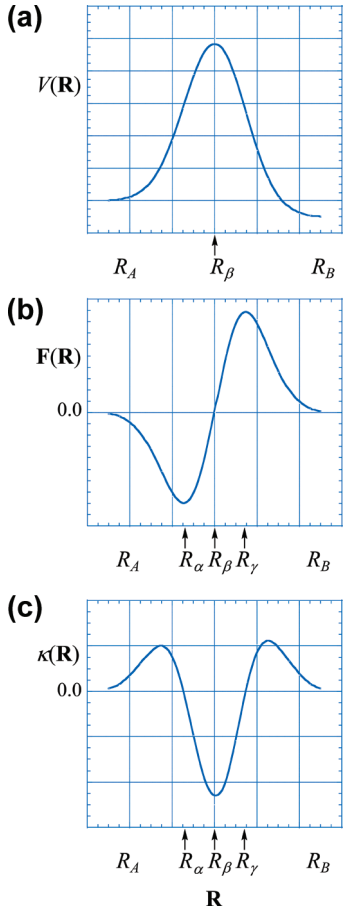

Figure 1. (a) Typical profile of the potential energy $V(\mathbf{R})$ of a one-step process A → B, plotted along the reaction coordinate **R**. R_A and R_B indicate equilibrium positions along **R** of reactants and products, respectively. In (b) and (c) are, respectively, the corresponding reaction force $\mathbf{F}(\mathbf{R})$ and reaction force constant $\kappa(\mathbf{R})$. At the points R_α and R_γ are the minimum and maximum of $\mathbf{F}(\mathbf{R})$; the transition state is at R_β. The zeroes of $\mathbf{F}(\mathbf{R})$ and $\kappa(\mathbf{R})$ are indicated.

states of the products. In the third region, these relax structurally to their final states. On the basis of such observations, the three regions are commonly designated as reactant ($R_A \rightarrow R_\alpha$), transition ($R_\alpha \rightarrow R_\gamma$), and product ($R_\gamma \rightarrow R_B$).

It should be noted that the preceding characterization of the three regions of a process focuses upon their dominant features; these are, however, not exclusive. There are certainly some electronic effects in the first and third regions and some structural changes in the second.

This discussion has been only in terms of the forward process, A → B. The reverse, B → A, can be treated in the same manner. However the vector **R** is then in the opposite direction, and $\mathbf{F}(\mathbf{R})$ will be the mirror image of Figure 1b, with its minimum at R_γ and its maximum at R_α. Reaction force analysis can also be applied to multistep processes, perhaps involving some intermediates. $\mathbf{F}(\mathbf{R})$ will then have correspondingly more minima and maxima.[16]

The activation barrier of the process in Figure 1 is $V(R_\beta) - V(R_A)$, where the point R_β is commonly identified as the transition state. In terms of Figure 1b, it follows that the activation barrier ΔE_{act} is the sum of two components

$$\begin{aligned}\Delta E_{act} &= V(R_\beta) - V(R_A) \\ &= [V(R_\beta) - V(R_\alpha)] + [V(R_\alpha) - V(R_A)] \\ &= \Delta E_{act,2} + \Delta E_{act,1}\end{aligned} \quad (3)$$

$\Delta E_{act,1}$ is primarily the energy needed to overcome the resistance to the structural changes in the first region of the process, from R_A to R_α, while $\Delta E_{act,2}$ supports the first stage of the transition to products, $R_\alpha \rightarrow R_\beta$.

One important consequence of decomposing ΔE_{act} into its two components is that it reveals how an external agent, such as a solvent or a catalyst, affects the rate of a process. Is its influence mainly upon the structural changes that occur between R_A and R_α and hence upon $\Delta E_{act,1}$, or is it upon electronic factors between R_α and R_β, that is, $\Delta E_{act,2}$? We have seen examples of both;[8,10,17] these will be discussed in a later section.

Reaction Force Constant. As can be seen in Figure 1c, $\kappa(\mathbf{R})$ is positive in the first and third regions, passing through zero at R_α and at R_γ. Like $V(\mathbf{R})$, $\kappa(\mathbf{R})$ is a scalar and has the same form for both the forward and the reverse processes.

A significant feature of $\kappa(\mathbf{R})$ is that it is negative throughout the entire transition region between R_α and R_γ, not just at the point R_β that corresponds to the maximum of $V(\mathbf{R})$.[5,6] In its focus upon the entire region, $\kappa(\mathbf{R})$ is fully in accord with the concept of Zewail and Polanyi, reached independently within the framework of transition-state spectroscopy, that there is a transition region that is a continuum of transient, unstable states.[20,21] The boundaries of that region are identified by $\kappa(\mathbf{R})$ as R_α and R_γ, the positions of the $\mathbf{F}(\mathbf{R})$ minimum and maximum.

Components of Reaction Energetics. We have already pointed out that the $\mathbf{F}(\mathbf{R})$ minimum at R_α divides the activation barrier into two components, $\Delta E_{act,1}$ and $\Delta E_{act,2}$. These are associated, respectively, with the initial structural changes between R_A and R_α and with the first stage of the transition to products, from R_α to R_β. The net energy change in the entire transition region is given by

$$\Delta E_{transition} = V(R_\gamma) - V(R_\alpha) \quad (4)$$

Finally, the energy released in the third region of the process, between R_γ and R_B, will be labeled $\Delta E_{relaxation}$ since a dominant feature of this region is the structural relaxation of the distorted products to their equilibrium states

$$\Delta E_{relaxation} = V(R_B) - V(R_\gamma) \quad (5)$$

The overall energy of the process, ΔE, is the sum of the contributions from the three regions

$$\Delta E = \Delta E_{act,1} + \Delta E_{transition} + \Delta E_{relaxation} \quad (6)$$

These various energy quantities are listed in Table 1 for a series of 16 reactions. The fact that these data were obtained at several computational levels, as indicated, will not affect the discussion since the values for different reactions will not be compared unless the calculations were carried out by the same procedure.

Table 1 shows that the S_N2 reaction of CH_3Cl with H_2O is promoted by aqueous solution through a lowering of the energy required for the structural phase of the activation, $\Delta E_{act,1}$; specifically, the initial stretching of the C−Cl bond is

DOI: 10.1021/jz101135y | J. Phys. Chem. Lett. 2010, 1, 2858–2862

Table 1. Components of Reaction Energetics, in kcal/mol

reaction	$\Delta E_{act,1}$	$\Delta E_{act,2}$	ΔE_{act}	$\Delta E_{transition}$	$\Delta E_{relaxation}$	ΔE	reference
$CH_3Cl + H_2O \rightarrow CH_3OH + HCl$ (g)[a]	39.1	27.5	66.6	0.8	−34.9	5.0	8
$CH_3Cl + H_2O \rightarrow CH_3OH + HCl$ (aq)[b]	32.6	26.2	58.8	2.0	−29.1	5.5	8
$CH_3CH{=}CH_2 + HCl \rightarrow CH_3CH(Cl)CH_3$ (g)[a]	10.5	29.2	39.7	4.8	−33.5	−18.2	10
$CH_3CH{=}CH_2 + HCl \rightarrow CH_3CH_2CH_2Cl$ (g)[a]	25.4	20.5	45.9	−6.4	−34.3	−15.3	10
$CH_3CH{=}CH_2 + HCl \rightarrow CH_3CH(Cl)CH_3$ (chl)[c]	16.1	11.0	27.1	−13.4	−33.5	−30.8	10
$CH_3CH{=}CH_2 + HCl \rightarrow CH_3CH_2CH_2Cl$ (chl)[c]	26.5	8.4	34.9	−12.5	−29.5	−15.5	10
$(H_3C)_3CCH_2ONO_2 \rightarrow (H_3C)_3COCH_2ONO$	44.7	24.6	69.3	−10.9	−43.5	−9.7	19
$(H_3C)_3SiCH_2ONO_2 \rightarrow (H_3C)_3SiOCH_2ONO$	18.9	14.1	33.0	−1.5	−57.4	−40.0	19
S=N−OH → HS−N=O	17.8	8.7	26.5	−1.4	−23.4	−7.0	5
HC(=O)SH → HC(=S)OH	22.35	10.40	32.75	−1.60	−19.23	1.52	4
HC(=O)C(=O)SH → HC(=O)C(=S)OH	25.82	9.90	35.72	−5.11	−16.22	4.49	4
thymine (keto → enol)	32.64	16.97	49.61	9.97	−23.51	19.10	17
thymine (keto → enol) (with Mg^{2+})	27.11	17.10	44.21	7.73	−34.39	0.45	17
$(O_2N)_3CH \rightarrow (O_2N)_2C{-}N(O)OH$	28.8	16.4	45.2	12.8	−28.2	13.4	18
picric acid (nitro → aci)	23.3	7.7	31.0	5.7	−2.8	26.2	18
1,4-dinitroimidazole (nitro → aci)	13.8	6.2	20.0	5.3	−2.7	16.4	18

[a] Gas phase. [b] Aqueous solution. [c] Chloroform solution.

facilitated.[8] In the keto/enol tautomerization of thymine, the effect of the catalyst Mg^{2+} is also in the structural region $R_A \rightarrow R_\alpha$.[17] In both cases, the external agent has very little influence upon $\Delta E_{act,2}$.

A contrasting situation is found in the Markovnikov addition of HCl to propene.[10] Chloroform solution actually hinders the initial structural changes, increasing $\Delta E_{act,1}$, but this is more than countered by a marked decrease in $\Delta E_{act,2}$, so that the total activation barrier is diminished. Another notable consequence is that $\Delta E_{transition}$ goes from endothermic (4.8 kcal/mol) to exothermic (−13.4 kcal/mol).

For the reactions in Table 1, $\Delta E_{act,1} > \Delta E_{act,2}$, with only one exception. The structurally dominated part of the activation usually requires more energy than the first stage of the transition to products. This suggests that a promoting agent (i.e., catalyst, solvent, etc.) should generally target the first region of a reaction, between R_A and R_α.

An interesting pattern that can be seen in Table 1 concerns the quantities $\Delta E_{act,1}$ and $\Delta E_{relaxation}$. Their magnitudes are, respectively, the energies corresponding to the structural changes in the reactants between R_A and R_α and in the products between R_γ and R_B. The pattern seen in Table 1 is $|\Delta E_{relaxation}| < \Delta E_{act,1}$ for endothermic reactions, that is, $\Delta E > 0$, and the opposite is seen for exothermic ones. In endothermic reactions, therefore, the structural changes in the reactants between R_A and R_α tend to involve more energy than those in the products between R_γ and R_B, with the reverse being true for exothermic reactions.

This observation could be another way of stating the Hammond−Leffler postulate,[22,23] according to which the transition state in an endothermic process resembles more the products and that in an exothermic reaction resembles the reactants. The reaction force $\mathbf{F}(\mathbf{R})$ defines unambiguously a transition region, beginning with distorted (or activated) reactants at R_α and ending with distorted (or activated) products at R_γ. What we are finding in Table 1 is that for most of the endothermic processes, the system at R_γ is closer in energy to the products than is the system at R_α to the reactants, and vice versa for exothermic processes. Our emphasis in this variation of the Hammond−Leffler postulate is not on the transition state but rather on the distorted reactants and products at the beginning and end of the transition region.

Diabatic Analysis. The characterization of the three regions of a process as reactant, transition, and product is empirical, based upon detailed studies of a series of reactions. However, the same qualitative description can be obtained by analysis in terms of diabatic functions.[24−32]

Assume that the potential energies of the reactants A and products B separately can be represented by two parabolic diabatic energy surfaces $V_A(\mathbf{R})$ and $V_B(\mathbf{R})$. If there were no electronic interaction between them, the parabolas would simply intersect at some point, as in Figure 2a, and there would be no conversion of reactants into products. When reaction does occur, however, the electronic coupling between reactants and products leads to a linking of the two curves, producing an adiabatic surface $V_{ad}(\mathbf{R})$ such as is shown in Figure 2b. The points R_a and R_c mark the onset of significant deviation of the adiabatic surface from the original diabatic parabolas. Since the curvature between R_a and R_c is opposite to that before R_a and after R_c, these are the inflection points of $V_{ad}(\mathbf{R})$. They indicate, therefore, the positions of the minimum and the maximum of the corresponding $\mathbf{F}_{ad}(\mathbf{R})$.

The picture that emerges from Figure 2b is that the reactants initially undergo structural changes ("reorganization" in the terminology of diabatic analysis) as they follow the reactant parabola from equilibrium at R_A to the point R_a. At R_a is the first inflection point and hence the $\mathbf{F}_{ad}(\mathbf{R})$ minimum for the linked parabolas. Between R_a and R_c, the transition from the reactant to the product parabola takes place. This is complete at R_c, the second inflection point, the $\mathbf{F}_{ad}(\mathbf{R})$ maximum. After R_c, the system follows the product parabola and relaxes to equilibrium at R_B.

DOI: 10.1021/jz101135y | J. Phys. Chem. Lett. 2010, 1, 2858–2862

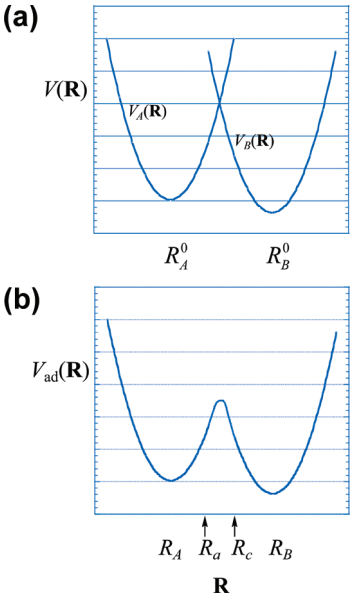

Figure 2. (a) Parabolic representations $V_A(\mathbf{R})$ and $V_B(\mathbf{R})$ of diabatic potential energies of reactants A and products B in the absence of any coupling between them. R_A^0 and R_B^0 indicate the equilibrium positions along reaction coordinate **R** of the noninteracting species. (b) $V_{ad}(\mathbf{R})$ adiabatic energy surface resulting from coupling of parabolic representations of reactants and products. R_A and R_B denote equilibrium positions of reactants and products; between R_a and R_c is the region of the strongest electronic coupling during the transition from A to B.

This description is clearly qualitatively similar to that relating to Figure 1b and c, which was based on the analysis of specific chemical processes. The points R_a and R_c in Figure 2b are the equivalent of R_α and R_γ in Figure 1. The linking of the reactant and product parabolas between R_a and R_c corresponds to the transition to the product region between R_α and R_γ. Finally, the structural reorganization taking place along the reactant parabola prior to R_a and along the product parabola after R_c is analogous to the structural changes before R_α and after R_γ.

The similarity between the results of reaction force and diabatic analysis will be demonstrated quantitatively in terms of two of the reactions in Table 1, shown below as eqs 7 and 8:

$$\mathrm{S{=}N{-}\,OH \rightarrow HS{-}\,N{=}O} \qquad (7)$$

$$\mathrm{HC(=O){-}\,SH \rightarrow HC(=S){-}\,OH} \qquad (8)$$

An adiabatic $V_{ad}(\mathbf{R})$ profile such as that in Figure 2b can be completely characterized in terms of four key diabatic parameters:[28,30,31]

(a) the change in the noninteracting equilibrium energies, $\Delta E_d = V_B(R_B^0) - V_A(R_A^0)$
(b) a measure V of the electronic coupling between reactants and products
(c) the reorganizational energy difference $\lambda_A = V_A(R_B^0) - V_A(R_A^0)$
(d) the reorganizational energy difference $\lambda_B = V_B(R_A^0) - V_B(R_B^0)$.

Note that $V_A(\mathbf{R})$ and $V_B(\mathbf{R})$ refer to the unperturbed reactant and product parabolas, as in Figure 2a. The complete

Table 2. Relative Locations of R_A, R_α, R_γ, and R_B from the Original Computed Data Compared to Values Obtained from Diabatic-Fitted Surfaces[a]

relative location	S=N−OH → HS−N=O		HC(=O)−SH → HC(=S)−OH	
	computed[b]	diabatic	computed[c]	diabatic
$R_A/(R_B - R_A)$	−0.42	−0.45	−0.53	−0.60
$R_\alpha/(R_B - R_A)$	−0.10	−0.13	−0.12	−0.16
$R_\gamma/(R_B - R_A)$	0.10	0.14	0.12	0.14
$R_B/(R_B - R_A)$	0.58	0.55	0.47	0.40

[a] In both cases, the transition states are set at $R_\beta = 0$. [b] Reference 5. [c] Reference 4.

Hamiltonian energy matrix in terms of the A and B diabatic electronic states is then given by

$$\mathbf{H} = \begin{pmatrix} E_0 + \lambda_A\left(\dfrac{R - R_A^0}{R_B^0 - R_A^0}\right)^2 & V \\ V & E_0 + \Delta E_d + \lambda_B\left(\dfrac{R - R_B^0}{R_B^0 - R_A^0}\right)^2 \end{pmatrix} \qquad (9)$$

where E_0 is a trivial energy offset; the reaction energy profile is the lowest-energy Born−Oppenheimer adiabatic surface $V_{ad}(\mathbf{R})$ obtained by diagonalizing H parametrically as a function of **R**.

For the proton-transfer reactions in eqs 7 and 8, the reactant and product states are hydrogen-bonded complexes, with well-characterized equilibrium positions at R_A and R_B, allowing easy representation in terms of adiabatic surfaces. We obtain these by constraining the parameters in eq 9 to reproduce the energies $V(R_A)$, $V(R_\alpha)$, $V(R_\beta)$, $V(R_\gamma)$, and $V(R_B)$ with the transition state located at $R_\beta = 0$. A gauge of the quality by which the interpolated surface reproduces the original reaction profile $V(\mathbf{R})$ is provided by comparison of the values of the reaction coordinate at which the critical points occur. The original and interpolated values of R_A, R_α, R_γ, and R_B relative to $(R_B - R_A)$ are shown in Table 2. There is good agreement. (The fact that $R_\alpha/(R_B - R_A) = -R_\gamma/(R_B - R_A)$ for each reaction is coincidental.) Thus, diabatic analysis for these proton-transfer reactions arrives independently at the same partitioning of a chemical process into three regions as was reached via the more general reaction force method.

Unifying Role of the Reaction Force. In an earlier study, we pointed out that the idea of a transition region that evolved from the reaction force has also come out of transition-state spectroscopy.[6] Now, we have drawn attention to the fact that an analogous interpretation emerges from diabatic analysis, first suggested by Horiuti and Polanyi in 1935[29] for proton-transfer reactions. It was shown to be more generally useful by Hush in 1953[25] and now forms the basis for all electron-transfer reaction modeling.[27] It matches the reaction force characterization of a chemical process as involving three regions, two dominated by structural changes and one that emphasizes electronic factors. In particular, both approaches offer the same type of qualitative insight into how solvent and substituent changes control reaction profiles and properties.

What we particularly wish to emphasize is the unifying role of the reaction force. It provides a general framework for

DOI: 10.1021/jz101135y | J. Phys. Chem. Lett. 2010, 1, 2858–2862

describing a chemical process that can encompass such diverse and independent concepts as the transition region being a continuum of transient, unstable states[20,21] (from transition-state spectroscopy), diabatic analysis,[24−32] and the Hammond−Leffler postulate.[22,23]

AUTHOR INFORMATION

Corresponding Author:

*To whom correspondence should be addressed.

ACKNOWLEDGMENT J.R.R. thanks the Australian Research Council and the National Computational Infrastructure for funding this research and Emeritus Professor Noel Hush for helpful discussions. A.T.L. gratefully acknowledges support from FONDECYT No. 1090460.

REFERENCES

(1) Fukui, K. The Path of Chemical Reactions — The IRC Approach. *Acc. Chem. Res.* **1981,** *14*, 363–368.
(2) Gonzalez, C.; Schlegel, H. B. Reaction Path Following in Mass-Weighted Internal Coordinates. *J. Phys. Chem.* **1990,** *94*, 5523–5527.
(3) Toro-Labbé, A. Characterization of Chemical Reactions from the Profiles of Energy, Chemical Potential and Hardness. *J. Phys. Chem. A* **1999,** *103*, 4398–4403.
(4) Toro-Labbé, A.; Gutiérrez-Oliva, S.; Murray, J. S.; Politzer, P. A New Perspective on Chemical and Physical Processes: The Reaction Force. *Mol. Phys.* **2007,** *105*, 2619–2625.
(5) Jaque, P.; Toro-Labbé, A.; Politzer, P.; Geerlings, P. Reaction Force Constant and Projected Force Constants of Vibrational Modes Along the Path of an Intramolecular Proton Transfer Reaction. *Chem. Phys. Lett.* **2008,** *456*, 135–140.
(6) Toro-Labbé, A.; Gutiérrez-Oliva, S.; Murray, J. S.; Politzer, P. The Reaction Force and the Transition Region of a Reaction. *J. Mol. Model.* **2009,** *15*, 707–710.
(7) Politzer, P.; Burda, J. V.; Concha, M. C.; Lane, P.; Murray, J. S. Analysis of the Reaction Force for a Gas Phase S_N2 Process: $CH_3Cl + H_2O \rightarrow CH_3OH + HCl$. *J. Phys. Chem. A* **2006,** *110*, 756–761.
(8) Burda, J. V.; Toro-Labbé, A.; Gutiérrez-Oliva, S.; Murray, J. S.; Politzer, P. Reaction Force Decomposition of Activation Barriers to Elucidate Solvent Effects. *J. Phys. Chem. A* **2007,** *111*, 2455–2458.
(9) Echegaray, E.; Toro-Labbé, A. Reaction Electronic Flux: A New Concept to Get Insights into Reaction Mechanisms. Study of Model Symmetric Nucleophilic Substitutions. *J. Phys. Chem. A* **2008,** *112*, 11801–11807.
(10) Burda, J. V.; Murray, J. S.; Toro-Labbé, A.; Gutiérrez-Oliva, S.; Politzer, P. Reaction Force Analysis of Solvent Effects in the Addition of HCl to Propene. *J. Phys. Chem. A* **2009,** *113*, 6500–6505.
(11) Jaque, P.; Toro-Labbé, A.; Geerlings, P.; De Proft, F. Theoretical Study of the Regioselectivity of [2 + 2] Photocycloaddition Reactions of Acrolein with Olefins. *J. Phys. Chem. A* **2009,** *113*, 332–344.
(12) Politzer, P.; Murray, J. S.; Lane, P.; Toro-Labbé, A. A Noteworthy Feature of Bond Dissocation/Formation Reactions. *Int. J. Quantum Chem.* **2007,** *107*, 2153–2157.
(13) Politzer, P.; Murray, J. S. The Position-Dependent Force Constant in Bond Dissociation/Formation. *Collect. Czech. Chem. Commun.* **2008,** *73*, 822–830.
(14) Murray, J. S.; Toro-Labbé, A.; Clark, T.; Politzer, P. Analysis of Diatomic Bond Dissociation and Formation in Terms of the Reaction Force and the Position-Dependent Reaction Force Constant. *J. Mol. Model* **2009,** *15*, 701–706.
(15) Toro-Labbé, A.; Gutiérrez-Oliva, S.; Concha, M. C.; Murray, J. S.; Politzer, P. Analysis of Two Intramolecular Proton Transfer Processes in Terms of the Reaction Force. *J. Chem. Phys.* **2004,** *121*, 4570–4576.
(16) Herrera, B.; Toro-Labbé, A. The Role of the Reaction Force to Characterize Local Specific Interactions That Activate the Intramolecular Proton Transfers in DNA Bases. *J. Chem. Phys.* **2004,** *121*, 7096–7102.
(17) Rincón, E.; Jaque, P.; Toro-Labbé, A. Reaction Force Analysis of the Effect of Mg(II) on the 1,3 Intramolecular Hydrogen Transfer in Thymine. *J. Phys. Chem. A* **2006,** *110*, 9478–9485.
(18) Murray, J. S.; Lane, P.; Göbel, M.; Klapötke, T. M.; Politzer, P. Reaction Force Analyses of Nitro-Aci Tautomerizations of Trinitromethane, the Elusive Trinitromethanol, Picric Acid and 2,4-Dinitro-1H-imidazole. *Theor. Chem. Acc.* **2009,** *124*, 355–363.
(19) Murray, J. S.; Lane, P.; Nieder, A.; Klapötke, T. M.; Politzer, P. Enhanced Detonation Sensitivities of Silicon Analogs of PETN: Reaction Force Analysis and the Role of σ-Hole Interactions. *Theor. Chem. Acc.* **2010**, DOI:10.1007/s00214-009-0723-9.
(20) Polanyi, J. C.; Zewail, A. H. Direct Observation of the Transition State. *Acc. Chem. Res.* **1995,** *28*, 119–132.
(21) Zewail, A. H. Femtochemistry: Atomic-Scale Dynamice of the Chemical Bond. *J. Phys. Chem. A* **2000,** *104*, 5660–5694.
(22) Leffler, J. E. Parameters for the Description of Transition States. *Science* **1953,** *117*, 340–341.
(23) Hammond, G. S. A Correlation of Reaction Rates. *J. Am. Chem. Soc.* **1955,** *77*, 334–338.
(24) Evans, M. G.; Polanyi, M. Inertia and Driving Force of Chemical Reactions. *Trans. Faraday Soc.* **1938,** *34*, 11–24.
(25) Hush, N. S. Quantum-Mechanical Discussion of the Gas-Phase Formation of Quinonedimethide Monomers. *J. Polym. Sci.* **1953,** *11*, 289–298.
(26) Marcus, R. A. Chemical and Electrochemical Electron-Transfer Theory. *Annu. Rev. Phys. Chem.* **1964,** *15*, 155–196.
(27) Marcus, R. A.; Sutin, N. Electron Transfers in Chemistry and Biology. *Biochim. Biophys. Acta* **1985,** *811*, 265–322.
(28) Reimers, J. R.; Hughes, J. M.; Hush, N. S. Modeling the Bacterial Photosynthetic Reaction Center 3: Interpretation of Effects of Site-Directed Mutagenesis on the Special-Pair Midpoint Potential. *Biochemistry* **2000,** *39*, 16185–16189.
(29) Horiuti, J.; Polanyi, M. Outlines of a Theory of Proton Transfer. *J. Mol. Catal. A: Chem.* **2003,** *199*, 185–197.
(30) Reimers, J. R.; Hush, N. S. A Unified Description of the Electrochemical, Charge Distribution, and Spectroscopic Properties of the Special-Pair Radical Cation in Bacterial Photosynthesis. *J. Am. Chem. Soc.* **2004,** *126*, 4132–4144.
(31) Schutz, C. H.; Warshel, A. Analyzing Free Energy Relationships for Proton Translocations in Enzymes: Carbonic Anhydrase Revisited. *J. Phys. Chem. B* **2004,** *108*, 2066–2075.
(32) Kraka, E.; Cremer, D. Computational Analysis of the Mechanism of Chemical Reactions in Terms of Reaction Phases: Hidden Intermediates and Hidden Transition States. *Acc. Chem. Res.* **2010,** *43*, 591–601.

DOI: 10.1021/jz101135y | *J. Phys. Chem. Lett.* **2010,** *1*, 2858–2862